Design and Analysis of a High Pressure Turbine Using Computational Methods for Small Gas Turbine Application

Article · December 2013

DOI: 10.1115/GTINDIA2013-3606

Prathapanayaka Rajeevalochanam
National Aerospace Laboratories

Kishore Kumar Sankara
Defence Research and Development Organisation

Proceedings of the ASME 2013 Gas Turbine India Conference
GTINDIA2013
December 5-6, 2013, Bangalore, Karnataka, INDIA

GTINDIA2013-3606

DESIGN AND ANALYSIS OF A HIGH PRESSURE TURBINE USING COMPUTATIONAL METHODS FOR SMALL GAS TURBINE APPLICATION

Kishor Kumar
CSIR-National Aerospace Laboratories
Bangalore, Karnataka, India

R. Prathapanayaka
CSIR-National Aerospace Laboratories
Bangalore, Karnataka, India

S. V. Ramana Murthy
DRDO-Gas Turbine Research Establishment
Bangalore, Karnataka, India

S. Kishore Kumar
DRDO-Gas Turbine Research Establishment
Bangalore, Karnataka, India

T. M. Ajay Krishna
BLDEA's PG Halakati College of Engineering
Bijapur, Karnataka, India

ABSTRACT
This paper describes the aerodynamic design and analysis of a high-pressure, single-stage axial flow turbine suitable for small gas turbine engine application using computational methods. The specifications of turbine were based on the need of a typical high-pressure compressor and geometric restrictions of small gas turbine engine. Baseline design parameters such as flow coefficient, stage loading coefficient are close to 0.23 and 1.22 respectively with maximum flow expansion in the NGV rows. In the preliminary design mode, the meanline approach is used to generate the turbine flow path and the design point performance is achieved by considering three blade sections at hub, mean and tip using the AMDC+KO+MK+BSM loss models to meet the design constraints. An average exit swirl angle of less than 5 degrees is achieved leading to minimum losses in the stage. Also, NGV and rotor blade numbers were chosen based on the optimum blade solidity. Blade profile is redesigned using the results from blade-to-blade analysis and through-flow analysis based on an enhanced Dawes BTOB3D flow solver. Using PbCFD (Pushbutton CFD) and commercially available CFD software ANSYS-CFX, aero-thermodynamic parameters like pressure ratios, aerodynamic power, and efficiencies are computed and these results are compared with one another. The boundary conditions, convergence criterion, and turbulence model used in CFD computations are set uniform for comparison with 8 per cent turbulence intensity. Grid independence study is performed at design point to optimize the grid density for off-design performance predictions. ANSYS-CFX and PbCFD have predicted higher efficiency of 3.4% and 1.2% respectively with respect to targeted efficiency of 89 per cent.

INTRODUCTION
With the evolution of commercial turbomachinery design codes, the task of designing the turbines has become cost effective in terms of time and money [1, 2, and 3]. Today's design codes include the optimization suite to arrive at the realistic design. Recently, NAL has procured the state-of-the-art turbomachinery design software for design and analysis of axial flow turbomachines available commercially from Concepts NREC Inc., INDIA. The design software has the capability to meet the comprehensive design requirements of these types of machines and is validated for steam and gas turbine engines as reported in literature [1]. There are three set of modules available in this code to carry out the 1D/2D/3D design and analysis along with multi-disciplinary optimization tool. The 1D module is used to start from preliminary design to final turbine map generation with the given set of design requirements. The 2D/3D module is used for blade profile design, blade-to-blade loading calculations, through-flow calculation and 3D CFD analysis. These modules are used in a rational manner in the process of design to demonstrate the principles in this field for effective design and are reported in this paper.

The overall design process of a gas turbine engine starts with a given set of specifications, which normally arises from market research or an understanding of specific customer requirements. There are three principle steps involved in turbine aerodynamic design process: preliminary design using meanline approach, through flow design, and airfoil design which is followed by a 3D CFD analysis in a typical computational environment.

In this paper, an attempt is made to carry out the aerodynamic design and analysis of a single stage, high pressure turbine using this code and redesign the blade profiles based on the computational out come with detail procedures to achieve proximity to realistic estimate of the aerodynamic parameters.

NOMENCLATURE

R	radial span, m
Z	axial distance, m
R_{theta}	profile circumferential point, m
T_{max}	maximum thickness, m
C_{ax}	axial chord, m
T_{41}	stage inlet total temperature, K
ΔT	temperature difference, K
C_p	specific heat at constant pressure, J/kgK
P_4	stage inlet total pressure, kPa
N	rotational speed, rpm
W_g	mass flow rate, kg/s
P	turbine aerodynamic power output, W
PR_{tt}	total-to-total pressure ratio
PR_{ts}	total-to-static pressure ratio
o	passage width, m
c	actual chord, m
s	blade pitch or spacing, m
p_{st}	static pressure, kPa
x	x-coordinate in axial direction
η_{tt}	total-to-total adiabatic efficiency, %
δ	rotor tip clearance, %
k	turbulence kinetic energy, J/kg
ω	specific turbulence dissipation rate, 1/s

Abbreviations

1D/2D/3D	One/Two/Three dimensional
AMDC	Ainley, Mathiesen, Dunham and Came
KO	Kacker and Okapuu
MK	Moustapha, Kacker, and Tremblay
BSM	Benner, Sjolander and Moustapha
CFD	Computational Fluid Dynamics
PbCFD	Pushbutton CFD
CSIR	Council of Scientific and Industrial Research
NAL	National Aerospace Laboratories
LE/TE	Leading/Trailing Edge
GATET	GAs Turbine Enabling Technologies
NGV	Nozzle Guide Vane
GTRE	Gas Turbine Research Establishment
CAD	Computer-Aided-Design
SST	Shear-Stress-Transport
DRDO	Defense Research & Development Organization
S-R	Stator-Rotor
N-S	Navier-Stokes
NACA	National Advisory Committee for Astronautics

MEANLINE DESIGN

The meanline design & analysis serves as the foundation for gas path preliminary design and performance estimation in a turbomachinery design cycle. The design of high-pressure turbine stage is carried out using the meanline design software based on the reduced-order, through-flow approach that balances all conservation properties from hub-to-tip and inlet to exit of each blade row, Concepts NREC's AXIAL^{TM}. This design module is used for preliminary and detailed design of axial turbomachines namely compressors, fans, pumps and turbines with built in working fluids. The software could be used to perform aerodynamic design with basic structural parameters computations in the initial design mode.

Baseline design specifications of a typical gas turbine stage are listed in Table 1.

Table1: Baseline high pressure turbine design specifications

Sl. No.	Parameter	Symbol	Units	Values
1	Rotational speed function	$N/\sqrt{T_{41}}$	$rpm/\sqrt{K}$	1399.7
2	Flow function	$W_g\sqrt{T_{41}}/P_4$	$kg\sqrt{K}/s.kPa$	0.152
3	Specific output function	$C_p\Delta T/T_{41}$	J/kgK	231.1
4	Total-to-total pressure ratio	PR_{tt}	[-]	2.77
5	Target efficiency	η_{tt}	%	89

The meanline design is carried out in three modes. These are the preliminary design mode, redesign mode and the analysis mode. The preliminary design mode involves the stage flow path design using inlet operating conditions of the turbine to meet the given geometric limitations and structural requirements. The working fluid, design speed, mass flow rate, inlet total pressure and temperature and the reference input data with partial/full admission fraction are specified. The inlet aerodynamic parameters, type of flow (subsonic /supersonic), flow profile from hub-to-tip are also specified. The minimum mass flow rate at the exit of turbine is specified to prevent overheating at this stage. One of the critical requirements of the preliminary design mode is to explore the design targets. This involves parametric study of the design specifications by choosing the flow coefficient, the stage loading coefficient, design total-to-static pressure ratio, targeted total-to-total adiabatic efficiency to get the desired performance. In the present case, number of stage is set to one. The flow path constraints are constant tip radius, type of blade sections (constant/variable), flow path limits (maximum hub/tip radius), inlet and exit swirl angles. Thus, the near optimum values of flow coefficient and load coefficient are determined and are close to 0.23 and 1.22 respectively. These values are chosen based on the near optimum pitch-to-chord ratio in between 1.33

and 1.43 for blades with inlet and exit absolute flow angle of zero degree and 70 degree respectively, to maintain the minimum blade profile loss as reported in [4]. Figure 1, shows the flow path contours of high-pressure turbine stage. In this design, the NGV row is choked and the rotor row is un-choked to extract the maximum possible energy in the stage. Once, the performance and analysis in this stage is arrived to be satisfactory, the flow path of the turbine is vetted and the redesign mode of module is activated to define input data for the NGV row and rotor row. This involves selection of blade profiles where in Pritchard airfoils are preferred in view of the blade profile designed with well defined 11 geometric parameters. Profiles are efficient and are widely used in the current small gas turbine engines. Standard profiles have wide range of operating incidence angle condition and standard performance curves could be used in the gas turbine. For specific application Pritchard profiles are preferred for the limited range of design incidence angles. In view of this, other possibilities such as NACA series or *foil genere* airfoils are not explored, though the choices are available in the design phase. Apart from the blade geometry, inlet and exit blade angles, blade profile geometric parameters at LE, TE, and mid-span geometry, loss models, blade solidity are input data in the redesign mode. The blade loss system is based upon the combined correlations of several highly renowned investigators: Ainley and Mathiesen [5], Dunham and Came [6], Kacker and Okapuu [7], and Moustapha, Kacker, and Tremblay [8] are part of the code.

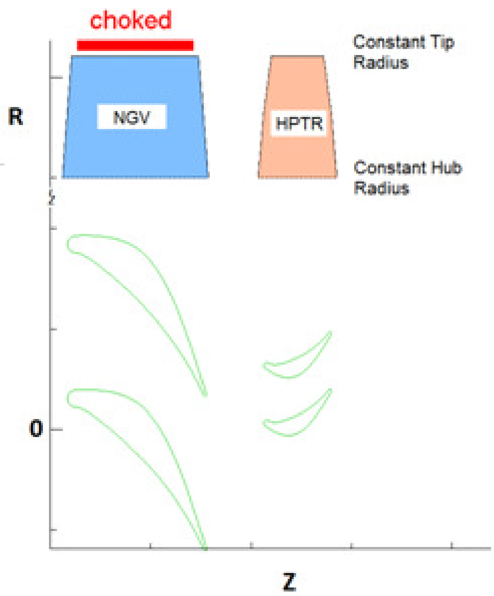

Figure 1 Meridional fluid flow path contour of turbine stage with mean section blade profiles [choked NGV row]

A lower value of reaction is emphasized for lower axial thrust on the bearings, higher margin of mechanical strength as well as to ensure the ease of starting the high pressure turbine stage in a typical small gas turbine engine application. The interrelation between reaction, blade numbers and loading are also explored using meanline analysis mode. The required low stage reaction is obtained by controlling the aerodynamic parameters like large acceleration and high turning of flow at the exit of NGV and high inlet relative velocity at the inlet of rotor. Apart from this, blade spacing and blade numbers could also play an important role and are explored sufficiently. The enthalpy based total-to-static reaction at the mean radius is close to 37 per cent.

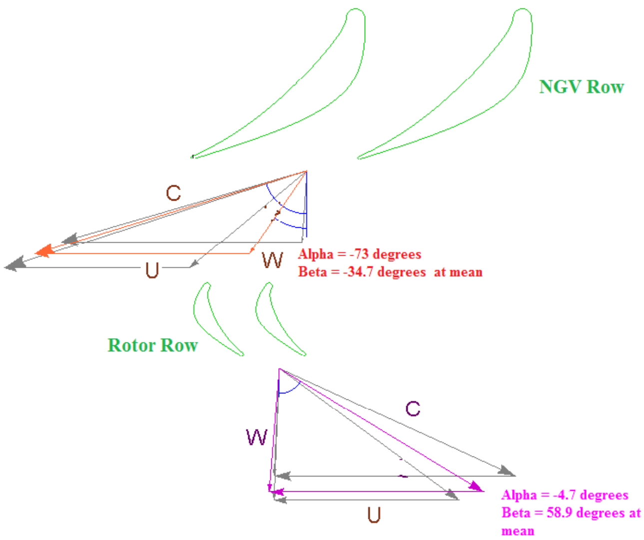

Figure 2 Velocity triangles at hub, mean and tip sections (values shown are at mean section) from AXIAL™

Figure 2 shows the velocity triangles for hub, mean, and tip sections across the rotor row. The meanline velocity triangles are determined by the choice of reaction and this in turn determines some of the principle features of blade design. The velocity triangles show that large acceleration and high turning of flow occurs at the exit of NGV blades, and high inlet relative velocity is seen to the rotor blades at mean section. The relative inlet velocity and Mach numbers are in the order of 380 m/s and 0.6 at hub radius respectively. This could result in slightly higher incidence loss, to overcome this; the LE and TE of the blades were designed with an incidence angle of zero degrees by re-staggering the blades, iteratively. In turbomachinery, which operates at high pressure, loss due to incidence is negligible as long as the incidence angle is zero or the flow is aligned with leading edge camber. However, in specific conditions, small negative incidence could result in slightly lower values of overall losses. Due to this, the incidence losses in the NGV and rotor blades are very low.

In selecting the low reaction design approach, the three dimensional character of the blade is also considered. At the hub the rotor blade speed is lower than at the tip, and therefore the blade loading and hence the flow deflection angle is found to be greater and in the order of 105 degrees at hub sections. This implied a lower reaction with positive values at hub and a higher reaction at the tip section.

Table 2 gives the summary of output details of turbine stage obtained from AXIAL™ design module. The centrifugal stress parameter is 3.7E07. Typical acceptable values for this parameter are between 1.9E07 to 3.8E07 m^2rpm^2, for materials such as Inconel 718. The efficiency of the turbine is more than 89 per cent for tip clearance of 150 microns. The efficiency decreased as the tip clearance was increased to 1.24 per cent of the blade height. With this clearance, the efficiency is 86.8 per cent. Since the profiles in meanline design is controlled by certain numerical values of blade geometry and are strictly 1D, there is scope for improvements to targeted efficiency in further design steps which has been carried out using AxCent™. Table 2a shows the loss coefficients and percentage efficiency decrement based on considered AMDC+KO+MK+BSM loss model for the initial blade shapes in the preliminary design mode.

Table 2: Turbine stage design output details from AXIAL™

Number of blades: NGV=19, ROTOR=51

Sl. No.	Parameters	Units	HPT Stage
1	Flow function	***kg√K/s.kPa***	0.15
2	Specific output function	***J.kg/√K***	226.5
3	Rotational speed function	***rpm/√K***	1399.7
4	Speed function	***m/s.√K***	13.6
5	Stage loading coefficient	-	1.22
6	Flow coefficient	-	0.23
7	Reaction (enthalpy, mean)	-	0.37
8	Reaction (pressure, mean)	-	0.29
9	Centrifugal stress function	m^2rpm^2	3.7E+07
10	Rotor exit relative Mach no.	-	0.88
11	Exit Reynolds no at mean NGV/rotor	millions	1.26 / 0.276
12	Hub-to-tip ratio	-	0.77
13	Running tip clearance	%	1.24
14	NGV throat area	m^2	0.004
15	Rotor throat area	m^2	0.0075

The secondary losses of NGV and rotor are from the actual pressure loss, where as the decrement in percentage of total loss, hence the contribution of secondary losses to the decrement in efficiencies can vary from NGV to rotor. The Table 2b shows the losses estimated for the modified profiles and it indicated that the losses in the NGV reduced to close to 0.095 and in the rotor to 0.020.

Table 2a: Loss coefficients based on AMDC+KO+MK+BSM loss model correlations

LOSS TYPE	**NGV**		
	Loss coefficients	Efficiency decrements	Kinetic energy loss
Profile loss	0.033	0.014	0.022
Secondary loss	0.090	0.037	0.057
Incidence loss	0.000	0.000	0.000
TE loss	0.008	0.003	0.005
LOSS TYPE	**ROTOR**		
	Loss coefficients	Efficiency decrements	Kinetic energy loss
Profile loss	0.047	0.015	0.032
Secondary loss	0.095	0.029	0.063
Incidence loss	0.000	0.000	0.000
TE loss	0.020	0.006	0.014
Leakage loss	0.086	0.026	0.057

BLADE PROFILE DESIGN AND ANALYSIS

The design of blades follows from the preliminary and through flow design process. The profile design methods are well known and are classified as direct or inverse methods. In the direct method, the profile design is optimized by incrementally changing the shape and evaluating the design at each step [9] whereas in the inverse method, the flow velocity distribution would be prescribed on suction and pressure surfaces. In the present case direct design method is adopted.

Table 2b: Loss coefficients for redesigned profiles, based on AMDC+KO+MK+BSM loss model correlations

LOSS TYPE	**NGV**		
	Loss coefficients	Efficiency decrements	Kinetic energy loss
Profile loss	0.023	0.014	0.022
Secondary loss	0.0655	0.0256	0.042
Incidence loss	0.000	0.000	0.000
TE loss	0.0068	0.0026	0.0053
LOSS TYPE	**ROTOR**		
	Loss coefficients	Efficiency decrements	Kinetic energy loss
Profile loss	0.047	0.015	0.032
Secondary loss	0.0747	0.0291	0.0357
Incidence loss	0.000	0.000	0.000
TE loss	0.020	0.006	0.014
Leakage loss	0.086	0.026	0.057

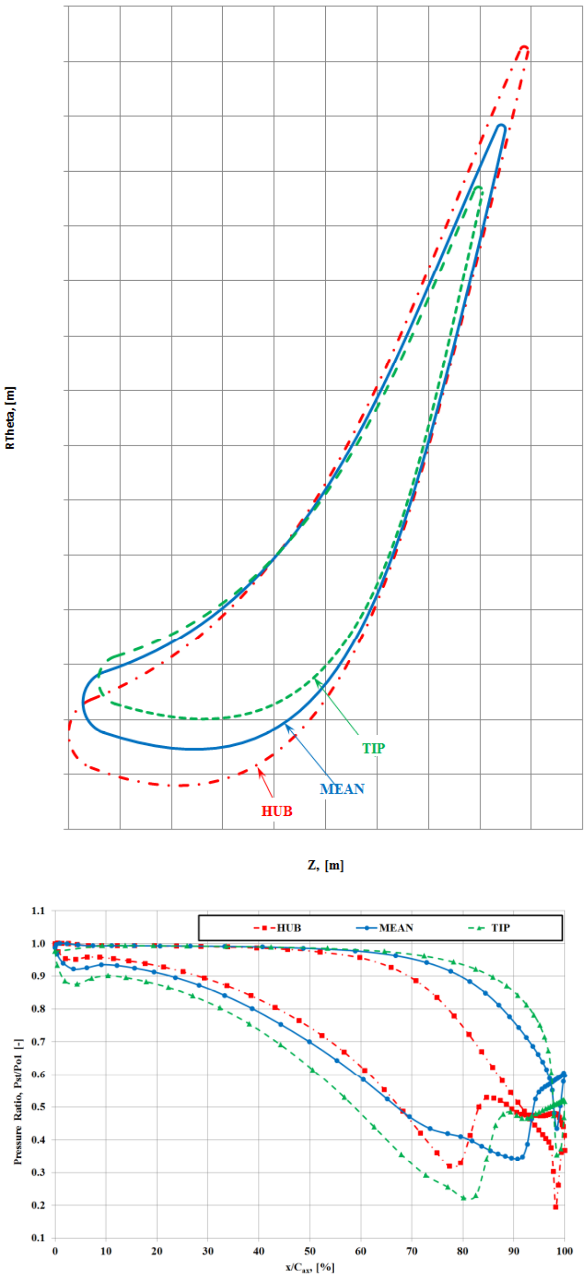

Figure 3 NGV profiles and loading at three sections

The design details obtained in AXIAL™ are transferred to the 2D design module called AxCent™ to create initial blade profiles, analyze the profiles using blade-to-blade solver to estimate the pressure distribution on the surfaces. This system integrates various blade shapes and stacking tools with interactive flow analysis that allow one to optimize the blade profiles in an iterative manner.

There are three different types of flow analysis approach available in this module they are blade-to-blade, through-flow and 3D N-S solver based PbCFD. In the present case, blade profiles are designed by considering three sections hub, mean and tip radius along the blade span. The profile design offers a variety of parameterized approach for constructing these 2D blade cross-sections. An improved Pritchard method [10] is provided as one standardized approach. However, more arbitrary blade profiles can be developed by the graphical control of Bezier curves for both the suction and pressure surface and the camber line thickness distributions. The fifth order polynomial is used to control the profile shape in this method. Better blade profiles can be designed rapidly by evaluating the blade loadings (i.e. static-to-total pressure ratio distribution on surfaces) and to adjust the surface curvatures at the selected blade span-wise sections. For each of the six sections, 3 each for NGV row and rotor row, the blade loading is computed using the blade-to-blade solver. The blade-to-blade solver is a 2D configuration of an enhanced Dawes BTOB3D flow solver [11]. Figure 3, shows the NGV profiles at three sections viz. hub, mean and tip locations along with the respective surface pressure distribution versus the axial distance from the leading edge. The NGV profiles are nearly constant exit flow angle. The NGV passage is designed for convergent area from LE to the throat to accelerate the flow. The region past the throat to TE is straight flow. It can be observed that the NGV is aft-loaded and the diffusion of the flow is after 80 per cent of the axial chord.

Figure 4, shows the rotor blade profiles at three sections viz. hub, mean and tip locations with respective surface pressure distribution as a function of axial distance from the leading edge. The pressure drop occurs uniformly over the blade passage. However, along the blade span it decreases from hub to tip as shown in figure. In the diffusion region of the rotor blade, the flow is decelerated due to boundary layer effects. This causes increase in the drag and significant loss of momentum; resulting in flow separation and much larger losses.

TURBINE GEOMETRY

The 3D turbine stage geometry model designed and redesigned as described in previous sections using AXIAL™ and AxCent™ modules is shown in Figure 5. The turbine has 19 NGVs and 51 rotor blades. It has a constant hub and tip radius with a hub-to-tip ratio of 0.767. The blade profiles are designed with variable geometry along the blade span. The rotor blade is twisted from hub to tip by an angle of 10 degrees could be observed in figure 5. The overall length of the turbine stage is around 60 mm. Table 3 shows the important geometrical dimensions extracted from AXIAL™ output file of the turbine at mean radius section for NGV and rotor rows.

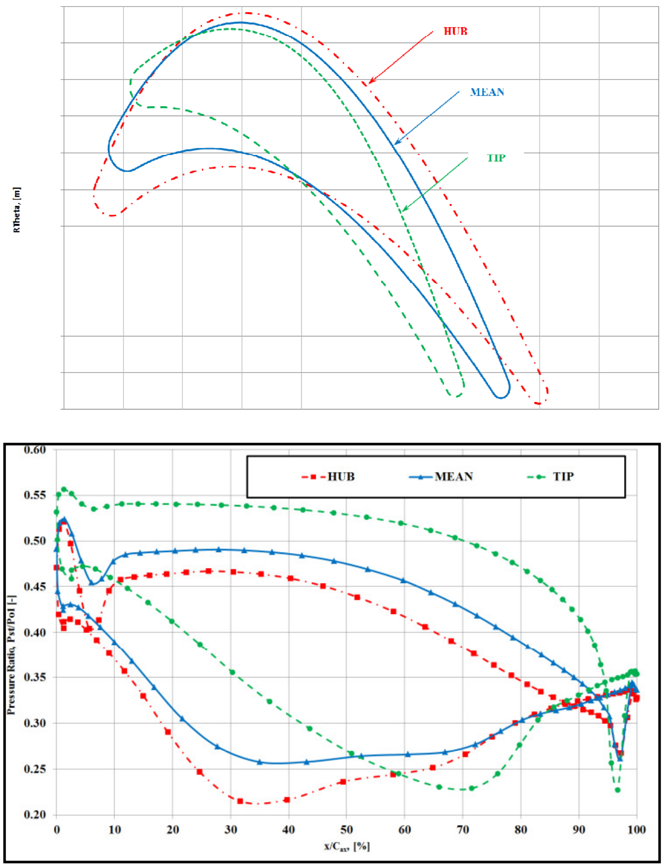

Figure 4 Rotor blade profiles and loading at three sections

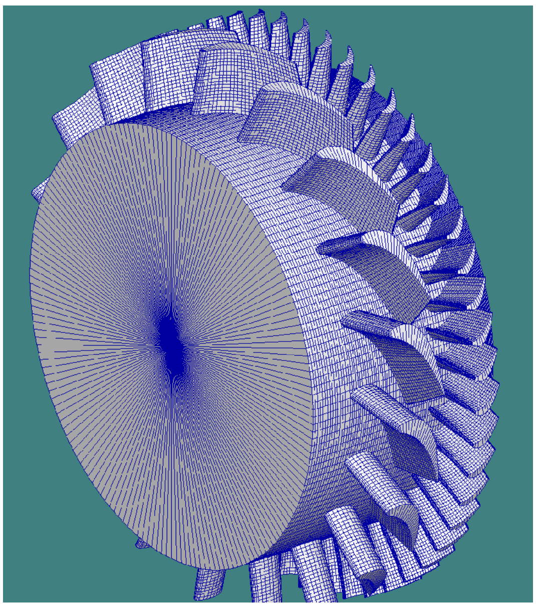

Figure 5 3D geometry of the turbine stage

Table 3: Important geometrical dimensions of turbine at mean radius extracted from AXIAL™

Sl. No.	Parameters	Units	NGV	ROTOR
1	o/s	-	0.81	0.91
2	Half wedge angle, inlet	*degrees*	3.46	3.45
3	Half wedge angle, exit	*degrees*	3.25	3.5
4	Stagger angle	*degrees*	-49.5	27.1
5	Blade inlet angle	*degrees*	0	-34.7
6	Blade exit angle	*degrees*	-73.0	58.9
7	T_{max}/c	*%*	0.182	0.22
8	c/s	-	1.35	1.31
9	Zweifel coefficient	-	0.64	0.97

CFD ANALYSIS

The 3D CAD model generated in AXIAL™ is transferred and used to perform the single blade passage 3D CFD analysis using two methods PbCFD in AxCent™ and ANSYS-CFX which are provided in the code. Table 4 shows the capabilities of the solver in both these methods adapted in the CFD analysis.

Table 4: Solver settings for CFD analysis

Sl. No.	Solver parameter	PbCFD	CFX
1	Equations	Dawes, multiblock	Compressible RANS
2	Turbulence model	SST, k-ω, second order	SST, k-ω, second order
3	Turbulence intensity	8 %	8 %

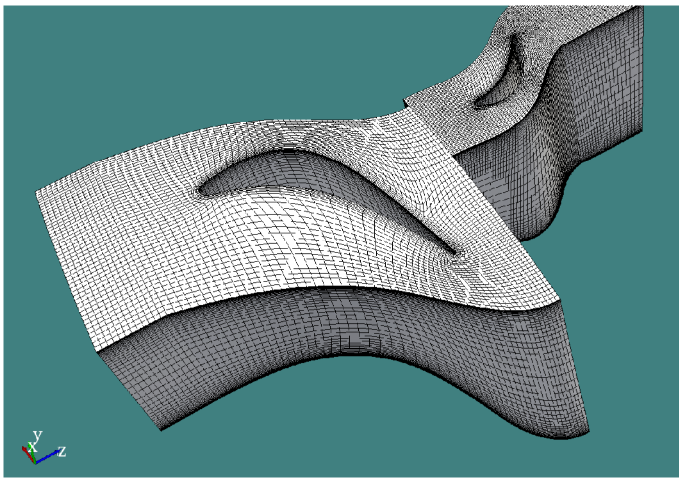

Figure 6a CFD Grids with O-H topology of the turbine stage for PbCFD

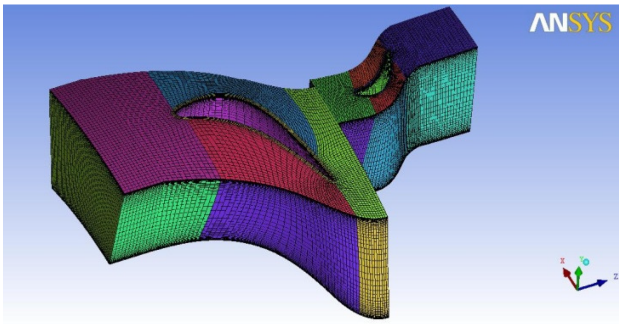

Figure 6b CFD Grids with O-H topology of the turbine stage for ANSYS-CFX

Instead of analyzing the complete row of NGV and rotor blades, axis-symmetric approach is used wherein only one flow path covering one blade row pitch is considered for analysis. Structured mesh is considered for the present analysis.
In order to optimize the mesh density, grid independence study is performed at design point using 0.11million, 0.196 million, 0.385 million and 0.77 million grids and then the optimized mesh size is utilized for off-design performance predictions.
The O-H topology grids are used with a grid density of 0.385 million for the steady state performance predictions as shown in Figures 6a and 6b. The Shear Stress Transport (SST), k-ω model with 8 percent turbulence intensity is used for the transport of turbulent shear stress as it accelerates the computations and sufficiently predicts the onset, the amount of flow separation under adverse pressure gradients. The result is taken for convergence criteria below 1E-05 and physical timescale of 60/N. The equations of fluid flow over a region of interest, with specified conditions on the boundary of that region.

Table 5: Boundary conditions

Sl. No.	Solver Parameter	PbCFD	CFX
1	Inlet conditions	P_4 and T_{41}	P_4 and T_{41}
2	Exit condition	p_{st}	p_{st}
3	Periodic conditions	Surfaces defining PS and SS side of domain	Surfaces defining PS and SS side of domain
4	No slip wall condition	Hub, tip and blade walls	Hub, tip and blade walls
5	S-R Interface	Circumferential averaging-Mixing Plane	Frozen rotor

Due to the subsonic characteristics, the selected parameter at the exit is free stream static pressure.
Periodic boundary conditions are used, since it is a simple mathematical boundary condition and allows only a small section of the full geometry to be modeled. All wall boundaries such as hub, tip and blade walls are considered as no slip walls. Table 5 above shows the comparison of the boundary conditions applied in the computational domain for both CFD methods.
In PbCFD, the stator-rotor interface is treated using circumferential averaging because NGV and rotor pitch being different and the flux balances between these interfaces could be accurate. The boundary layer grids are generated and used in the analysis, achieving a y+ value of 1 for the final converged iteration.
Figure 7 shows the computational domain in ANSYS-CFX with the applied boundary conditions. In this case, frozen rotor model is invoked in the mixing plane because of its advantages of wake passing capability without much distortion. One circumferential pitch covering two blades in the stator and one circumferential pitch in the rotor covering two blades are used for the analysis.

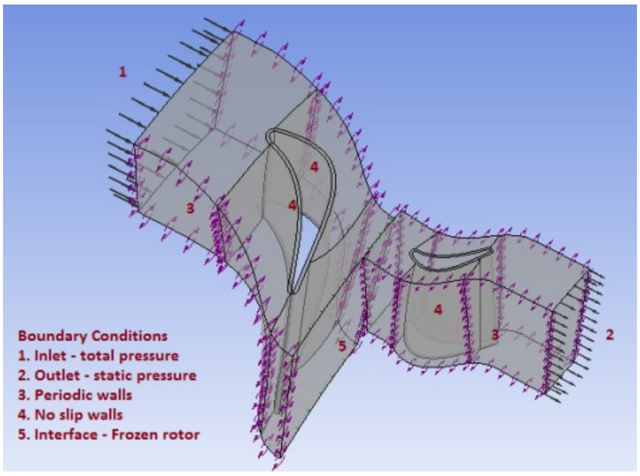

Figure 7 Computational domain and boundary conditions definition

The boundary layer grids are generated and used in the analysis, achieving a y+ value of 10 for the final converged iteration. Fluid is exhaust gas from combustion process of specific heat at constant pressure 1220 J/kg K and ratio of specific heat 1.3.
The results of grid independence study for coarse, medium, fine, and very-fine mesh is listed in Table 6.

Table 6: PbCFD Grids independence study (coarse, medium, fine and very fine mesh density)

Sl. No.	Cells in K direction	No. of Grids	η_{tt} [%]
1	13 (Coarse)	110037	86.3
2	25 (Medium)	196550	88.4
3	*49 (Fine)*	*385238*	*89.8*
4	79 (Very-fine)	770476	89.4

The performance remained nearly constant beyond grid density of 0.385 millions, and hence this grid size was chosen for off-design performance predictions.
Design and off-design performance map points are predicted by varying total-to-static pressure ratio at the exit of the stage.

RESULTS & DISCUSSION

The aerodynamic parameters of the stator and rotor rows are summarized in Table 7a and 7b for hub, mean and tip sections. The inlet flow angle to the stage is axial with zero incidence angles. The absolute Mach number at the NGV exit is 1.04 at mean radius. Figures 8a, 8b and 8c show the relative Mach number contours at hub, mean, and tip section respectively. It can be observed that the exit Mach number of 1.19 occurs at the hub section for the NGV row indicating choked flow in this row (red color region at the throat), while at the mean and tip section the respective values are 1.04 and 0.92. The rotor is operating with un-choked flow as the flow is subsonic over the blade passage. The average exit swirl angle is less than 5 degrees.

Table 7a: NGV aerodynamic parameters

Sl. No.	Parameters	Hub	Mean	Tip
1	Inlet flow angle	0	0	0
2	Inlet Mach no.(absolute)	0.162	0.162	0.162
3	Exit total pressure	1300	1323	1339
4	Exit static pressure	601	720	825
5	Exit total temperature	1349	1349	1349
6	Exit static temperature	1224	1169	1203
7	Exit velocity(absolute)	740	663	596
8	Exit flow angle(absolute)	-72.2	-73.0	-73.9
9	Exit Mach no.(absolute)	1.14	1.0	0.89

Table 7b: Rotor aerodynamic parameters

Sl. No.	Parameters	Hub	Mean	Tip
1	Inlet flow angle	-72.1	-73.0	-73.9
2	Inlet relative Mach No.	0.55	0.35	0.25
3	Exit relative total pressure	673	715	773
4	Exit static pressure	443	443	443
5	Exit relative total temperature	1176	1191	1191
6	Exit static temperature	1066	1064	1065
7	Exit relative flow angle	53.7	58.9	65.5
8	Exit relative velocity	519	557	603
9	Exit relative Mach No.	0.82	0.88	0.95
10	Exit swirl angle	-2.3	-4.7	-2.75

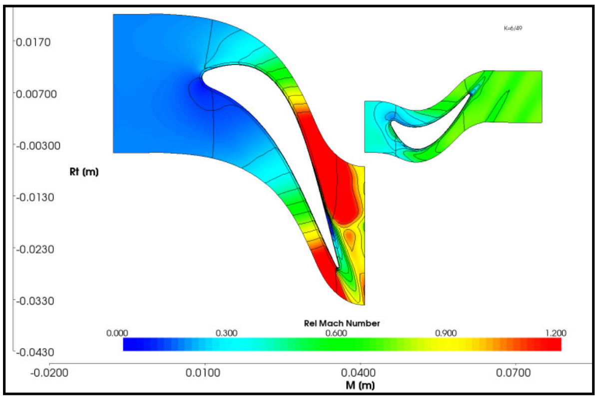

Figure 8a Relative Mach number contours at hub section

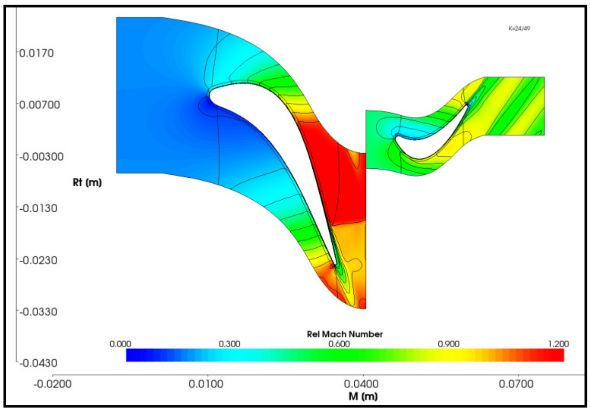

Figure 8b Relative Mach number contours at mean section

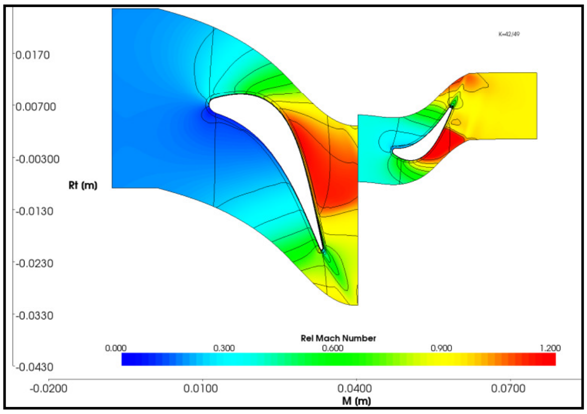

Figure 8c Relative Mach number contours at tip section

Figures 9a and 9b show the comparative study of the turbine power output versus total-to-total pressure ratio at the design and off-design points using above methods. The off-design performance is predicted at 70 %, 80%, 90% and 110 % of the design speed with the variation of total-to-static pressure ratio between 2 and 3.5 in increments of 0.2. The PbCFD predictions indicated that the desired performance of the turbine will be achieved using the chosen design input parameters. However, the ANSYS-CFX predictions indicate the higher power output for the given pressure ratios in comparison to the other methods.

Figures 10a and 10b show the comparative study of the turbine total-to-total efficiency as a function of total-to-total pressure ratio using the above methods at the design and off-design points. The design point total-to-total efficiencies are 86.6 %, 90.1% and 92.1 % using the meanline, PbCFD and CFX respectively. These respective efficiencies are 2.7 % less, 1.2 % more and 3.4 % more than that of the targeted efficiency as shown in Table 7. Hence, the PbCFD and CFX results gave sufficiently good predictions in comparison to the meanline code since the blade profiles were optimized for better performance in 2D module. The boundary layer grid resolution used in PbCFD method achieving y+ value closer to 1 could be one of the possible reasons for predicting better performance using PbCFD in comparison to ANSYS-CFX where the y+ value is closer to 10 and turbulence model invoked in the predictions.

It can be observed from the figure that meanline prediction shows the gradual increase in efficiency and reaches a maximum of 86.8 per cent at design point and decreased gradually thereafter.

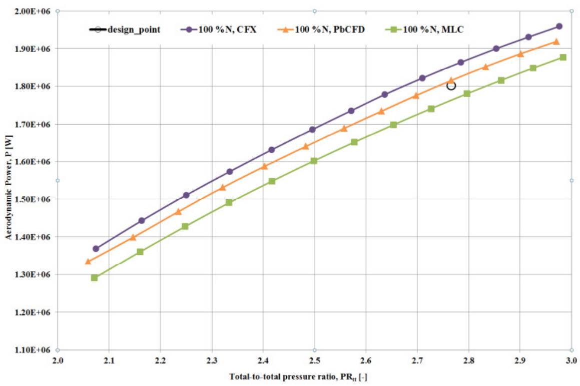

Figure 9a Comparison of power output at design speed

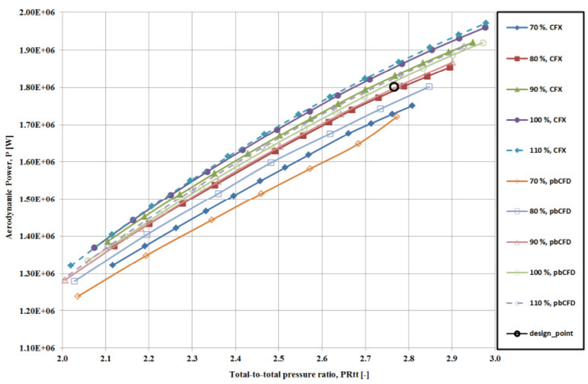

Figure 9b Power output of the turbine stage at off-design points

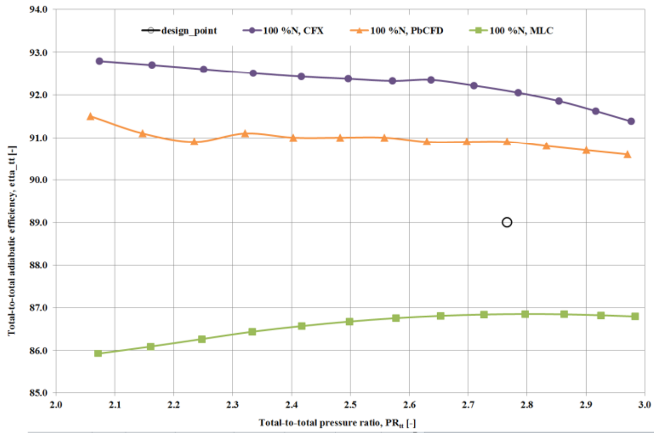

Figure 10a Comparison of efficiency at design speed

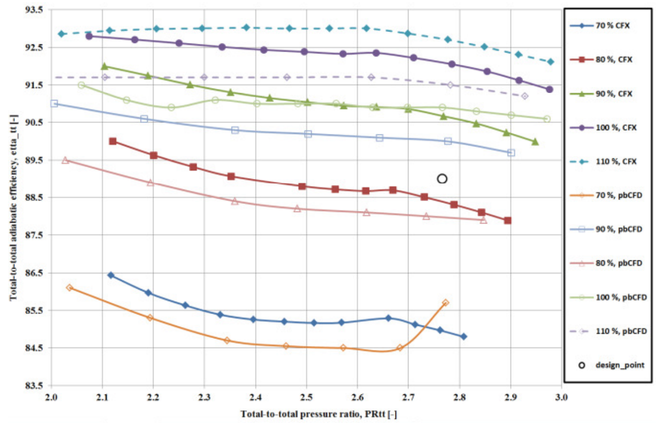

Figure 10b Off-design efficiency map of the turbine stage

Table 8: Comparison of turbine performance output at design point using 3 methods

Methods	Meanline		PbCFD		ANSYS-CFX	
Design targets	output	% deviation	output	% deviation	output	% deviation
PR_{tt}= 2.77	2.77	0.0	2.765	0.18	2.757	0.47
η_{tt} =89	86.8	2.5	90.1	1.2	92.1	3.4
P=1801.7 kW	1765	-2.02	1834	1.78	1860	2.9

Figure 11 shows the variation of the mass flow parameter with respect to the static-to-static pressure ratio at different operating speeds. The flow is nearly chocked for pressure ratio beyond 3.1 corresponding to total-to-total pressure ratio of 2.78. At design speed, the mass flow increases gradually for the range of pressure ratio and reaches the maximum up to design pressure ratio. Thereafter, the slope of the curve remains nearly constant.

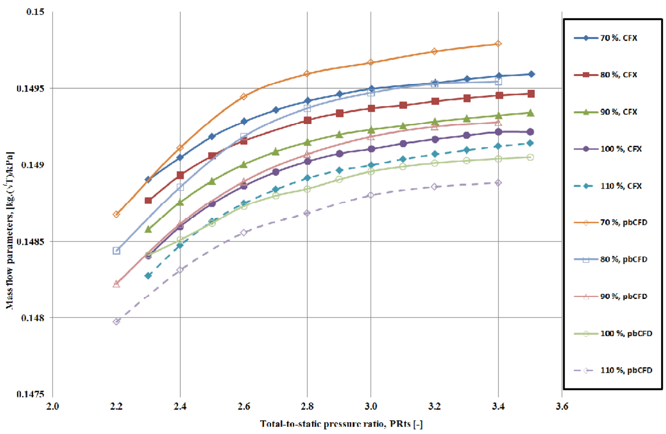

Figure 11 Off-design mass flow map of the turbine stage

CONCLUSIONS

A computational design and analysis is carried out for a high pressure small gas turbine stage using the state of the art turbomachinery design code available at NAL. Preliminary design of turbine stage carried out using meanline design module AXIAL™ to obtain the stage design parameters taking in to account the baseline design requirements and geometrical constraints.

Pritchard blade profiles are used for both stator and rotor in this step. The selected loss model predicts 0.13 and 0.24 overall loss in the stator and rotor respectively. The blade profiles were then modified using the Bezier profile curves to optimize the blade shape as well as re-stagger of blade resulted in reduction of overall loss to 0.095 in NGV and 0.20 in rotor.

The total-to-total adiabatic efficiency at design point predicted by PbCFD and CFX are 90.1 % and 92.1% respectively, and the experimental validation of these parameters is future scope of study.

ACKNOWLEDGMENTS

The author(s) wish to thank the Head, Propulsion Division and Director, CSIR-NAL, Bangalore and Director, DRDO-GTRE, Bangalore for permission to publish the research work. We are grateful to the GATET, DRDO-GTRE, Bangalore for funding support in the procurement of the axial turbomachinery design code. Author(s) also thank Mr. S. J. Krishnamurthy and Dr. M. V. A. Murthy for their valuable guidance and suggestions.

REFERENCES

[1] Dubitsky Oleg et. al., 2003. "The Reduced Order Through-flow Modeling of Axial Turbo-machinery", Proceedings of the International Gas Turbine Congress, Tokyo.

[2] Turner M. G. et. al. 2011. "A Turbomachinery Design Tool for Teaching Design Concepts for Axial-Flow Fans, Compressors, and Turbines", *Journal of Turbomachinery*, **133,** pp. 031017-1-12.

[3] Leonid Moroz et. al. 2007, "Advanced Gas Turbine Concept, Design and Evaluation Methodology, Preliminary Design of Highly Loaded low Pressure Gas Turbine of Aircraft Engine", Proceedings of the International Gas Turbine Congress, Tokyo.

[4] Horlock, J. H., 1958. "Axial Flow Turbine", Butterworth, London, p 89.

[5] Ainley, D. G., and Mathiesen, G. C. R., 1951. "A Method of Performance Estimation for Axial Flow Turbines", British ARC, R & M 2974.

[6] Dunham, J., and Came, P.M., 1970. "Improvements to the Ainley/Mathieson Method of Turbine Performance Prediction", *Journal of Engineering for Power*, pp 252-256.

[7] Kacker, S. C., and Okapuu, U., 1981. "A Meanline Prediction Method for Axial Flow Turbine Efficiency", *Journal of Engineering for Power*, **103**, No.1.

[8] Moustapha, S. H., Kacker, S. C., and Tremblay, B., 1990 "A Meanline Prediction Method for Axial Flow Turbine Efficiency", *Journal of Turbomachinery*, pp. 267-276, ASME Paper 89-GT-284.

[9] Japikse, D., 2002. "Developments in Agile Engineering for Turbomachinery," The 9th International Symposium on Transport Phenomena and Dynamics of Rotating Machinery", Honolulu, HI.

[10] Goel S., 2009 "Turbine airfoil Optimization Using Quasi-3D Analysis Codes", *International Journal of Aerospace Engineering*, **2009**.

[11] Dawes W. N. 1992. "Towards improved through flow capability: The use of 3D viscous flow solvers in a multistage environment", *Journal of Turbomachinery*, **114**, no.1.

[12] AXIAL™ User Manual, Concepts NREC Inc.

[13] AxCent™ User Manual, Concepts NREC Inc.

[14] ANSYS CFX-14; ANSYS CFX release 14